ARTICLES

Electron Spin Polarization Transfer and Radical-Triplet Pair Polarization in Nitroxide−C_{60} Derivative Systems

Elena Sartori, Antonio Toffoletti, and Carlo Corvaja*

Department of Physical Chemistry, University of Padova, via Loredan, 2, I-35131 Padova, Italy

Luigi Garlaschelli

Department of Organic Chemistry, University of Pavia, via Taramelli, 10, I-27100 Pavia, Italy

Received: June 19, 2001

Nitroxide free radical/[60]fullerene derivative liquid solutions photoexcited by visible laser pulses are investigated by time-resolved EPR. Both radical and triplet excited fullerene spin-polarized EPR signals are observed. Their time evolution is examined in terms of CIDEP effects due to electron spin polarization transfer from the initially polarized triplet to the nitroxide and to spin polarization generated by the radical triplet pair mechanism. Radical and triplet spin relaxation times and rate constants for the processes of polarization transfer and radical triplet pair mechanism are obtained.

Introduction

Since the earliest observations in the 1970s, electron spin polarization in chemical and photochemical reactions has been exploited in order to have detailed information on the mechanism of radical reactions.

Spin polarization is a deviation of spin sublevels population from the thermal equilibrium value. It is detected as an anomalous EPR line intensity: lines in enhanced absorption (A) and in emission (E) are recorded. The acronym CIDEP for chemical induced dynamic electron polarization is used for referring to this phenomenon.[1−3]

Several mechanisms are responsible for CIDEP. The most important are the triplet mechanism (TM),[4] the radical pair mechanism (RPM),[5−7] the radical triplet pair mechanism (RTPM),[8,9] and the direct polarization transfer from a polarized species. Usually the last phenomenon takes place from an excited triplet state to a free radical, but polarization transfer from a free radical to a second one was also observed.[10]

TM gives rise to EPR spectra in net absorption or emission, that is spectra in which all lines have the same polarization.

The most important contribution to RPM arises from the mixing of the singlet S with the triplet T_0 component due to differences in Larmor frequency because of unequal *g* factors or hyperfine coupling. When the radicals have the same *g* factor, RPM gives rise to spectra with a multiplet effect: low field hyperfine lines in absorption and high field ones in emission (A/E) or vice versa (E/A), depending on the singlet or triplet character of the precursor and on the sign of the product between hyperfine coupling constant and *J*. This pattern is superimposed to a net effect if the radical pair partners have different *g* factors, or if the $S/T_{\pm1}$ mixing is important.

RTPM is similar to RPM but takes place when a triplet excited molecule interacts with a free radical that may even be a stable one. This mechanism was introduced 10 years ago[8] when it was realized that the well-known phenomenon of triplet quenching by free radicals[11−14] could produce spin polarization. Most of the published studies refer indeed to the spin polarization of nitroxide radicals,[9,15−22] but even other polarized free radicals have been observed.[9] RTPM was also invoked for explaining the polarization effects observed in photoexcited single crystals containing free radical impurities or spin $^1/_2$ defects,[23] and more recently in molecular systems containing a triplet precursor and a free radical covalently linked,[24] connected by a coordination bond,[25] bound to a molecular template,[26] or linked in a host−guest complex.[27]

RTPM occurs because of the selective mixing of the pair quartet state Q with the pair doublet state components $D_{\pm1/2}$, caused by electron spin dipolar and hyperfine interactions. This mechanism gives net A or E spectra, as well as multiplet effects, depending on the sublevels of the pair quartet, which are prevalently mixed. When $Q_{\pm3/2}$ levels are involved, one has net polarization, while a multiplet effect is observed if the mixing involves the $Q_{\pm1/2}$ substates. In some cases, the spectrum shows multiplet polarization superimposed over net polarization.[9]

It should be noted that RTPM does not require spin polarization of the triplet partner. In irradiated solutions containing a free radical and a spin-polarized triplet, electron spin polarization transfer (ESPT) occurs from the excited triplet molecule to the free radical.[28−30] Its action was clearly demonstrated by the opposite polarization displayed by TEMPO radicals in the presence of triplet excited Zn and Cd porphyrines (ZnTPP, ZnOEP, CdTPP) or H_2 and Mg porphyrines (H_2TPP, H_2OEP MgTPP). The radical EPR lines occur in net absorption or emission according to the polarization of the triplet.[30,31] Triplet excited H_2 and Zn phthalocyanines and TEMPO radical

* Corresponding author. Telephone: ++39-049-8275684. Fax: ++39-049-8275135. E-mail: c.corvaja@chfi.unipd.it.

10.1021/jp0123280 CCC: $20.00
Published on Web 11/10/2001

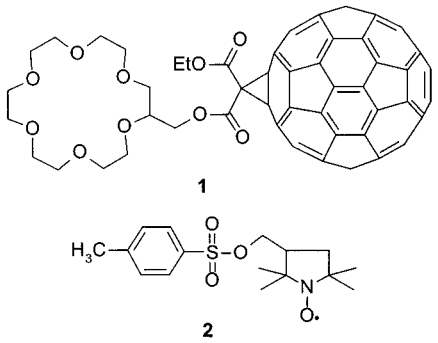

Figure 1. Molecular structures of the [60]fullerene crown ether and of the nitroxide radical, *p*-toluensulfonic ester of 3-(hydroxymethyl)-[2,2,5,5-tetramethylpyrrolidine-1-oxyl].

behave in the same way.[32] More recently, a quantitative study of ESPT and RTPM in triplet radical systems was carried out by FT-EPR.[33]

In the cases considered so far the spin dynamics of the system was inferred mostly from the analysis of the time evolution of the free radical signal, since the triplet partner of the RTP was not observed or its line intensity was too low. An exception is provided by a paper concerning triplet C_{60} and TEMPO where both triplet and radical signals were simultaneously recorded with similar signal-to-noise ratios.[19] However, in this case no ESPT effect is present.

In the course of our TR-EPR studies of photoexcited fullerene derivatives we have examined a system consisting of a triplet excited [60]fullerene crown ether **1** and a nitroxide radical bearing an alkylammonium group. The latter couples to the crown ether and forms a host−guest complex, which was observed in its quartet state generated by the coupling of the radical and triplet spins.[27] No quartet was observed when the *p*-toluensulfonic ester of 3-(hydroxymethyl)-[2,2,5,5-tetramethylpyrrolidine-1-oxyl] (**2**) (see Figure 1) was used as a radical species. In this case the TR-EPR spectrum shows strong polarized signals of both triplet and radical with interesting features, which could be analyzed in detail.

We will show that the observed features, including a remarkable multiplet effect, can be explained by assuming spin polarization deriving from ESPT and RTPM.

Other bulky C_{60} derivatives (methano[60]fullerenes variously substituted on malonic carbon) interacting with nitroxides, whose spectra will not be shown here, displayed analogous behavior.

Detailed analysis of the EPR signal time evolution of both partners was performed, giving the kinetic parameters characterizing the different processes.

Experimental Section

[60]Fullerene crown ether **1** was synthesized according to the procedure already described.[27] The *p*-toluensulfonic ester of 3-(hydroxymethyl)-[2,2,5,5-tetramethyl-pyrrolidine-1-oxyl] (**2**) was prepared as previously described.[34]

Solutions of **1** and **2** (2 mM) in $CHCl_3$ (Fluka) placed in quartz tubes of 2 mm inner diameter were carefully degassed by several freeze−pump−thaw cycles.

The illumination of the samples was performed by 20 ns 580 nm light pulses from a Lambda Physik FL2000 dye laser pumped by an excimer laser Lambda Physik LPX100.

The TR-EPR spectra were recorded without field modulation with a Bruker ER 200 D X-band spectrometer. The overall time resolution of the system is estimated to be 150 ns.

The transient EPR signals, generated by the laser pulses on the microwave diode detector, are amplified by a preamplifier (bandwidth: 20 Hz to 6.5 MHz) and collected by a digital oscilloscope (LeCroy 9450A), triggered by the laser pulse. For each value of the static field, 200 transient signals are averaged. 2D-TR-EPR spectra are obtained by sweeping the field and transferring the averaged transients recorded at each field address to a PC, where they are treated with a custom-made software. To correct for the cavity response to the laser perturbation, an off-resonance signal is subtracted from the transients recorded at all the field positions.

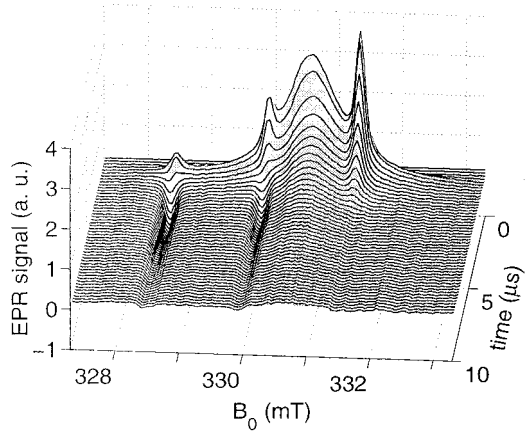

Figure 2. 2D-TR-EPR spectrum of a 2 mM solution of **1** and **2** in $CHCl_3$, at 260 K. The microwave power is 60 mW. Data were collected as a series of transient signals at different B_0 positions. However, to make the figure clearer, the data are displayed as a collection of spectra corresponding to different time delays.

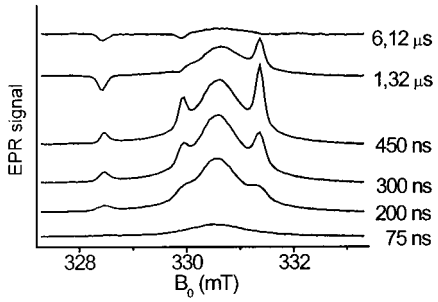

Figure 3. Sections of the 2D-TR-EPR spectrum in Figure 1 at increasing time delays after the laser pulse.

Results

Figure 2 shows the complete 2D-TR-EPR spectrum recorded by laser photoexcitation of a 2 mM $CHCl_3$ solution of **1** and **2**, at 260 K.

Figure 3 shows sections of the data surface taken at increasing time delays after the laser pulse. In the first instants after the light absorption, the spectrum consists of a single broad line with $\Delta B = 1.6$ mT, which is attributed to **1** in the excited triplet state. The same line is recorded if **2** is absent. At longer time delays, other features appear, consisting of three lines at the magnetic field positions corresponding to the EPR transition of **2**, split by the ^{14}N hyperfine interaction ($g = 2.0057$, $a_N = 1.5$ mT).

In the section taken at 200 ns delay, they appear as small bumps, approximately of the same intensity, over the broad line. The spectrum can be fitted by a sum of four Lorentzian lines, one of them being the broad line. A Gaussian line shape gives a worse fitting, indicating that the homogeneous contribution to the line width overcomes the inhomogeneous one. At still longer delays the nitroxide lines become more evident and they assume different intensities, the high field one being always in absorption, while the central field and the low field lines eventually assume an emissive character.

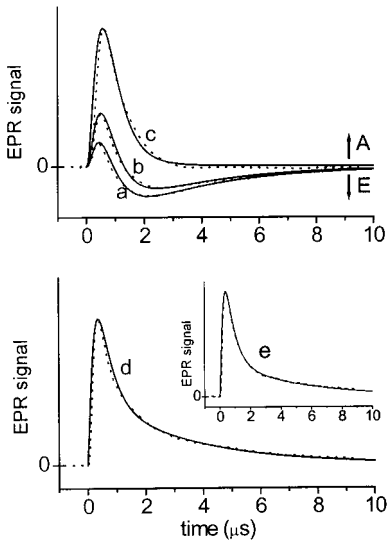

Figure 4. Sections of the 2D-TR-EPR spectrum in Figure 2 at specific field values corresponding to the maxima of (a) nitroxide low field line, (b) nitroxide central line, (c) nitroxide high field line, and (d) triplet line. (e) Time evolution of the triplet line recorded by illuminating **1** in the absence of free radical. Solid lines represent the time evolution calculated according to the mathematical model described in the Discussion. The calculated values were scaled so as to fit the experimental signal. Two different scaling factors had to be used for the radical lines and the triplet one. This is due to the fact that the latter is not completely homogeneous as assumed in the modified Bloch equations.

Figure 4 shows sections taken at specific field values, corresponding to the maxima of the spectral features discussed above. They represent the time evolution of the individual EPR transitions. For the central and high field hyperfine components of the radical spectrum, which are overlapped with the triplet line, the sections are displayed after having subtracted the contribution of the triplet. The inset shows a section of a 2D-TR-EPR spectrum obtained from a solution of **1** without radical. The best fit curves (solid lines) obtained by the theoretical model discussed in the next section are displayed as well.

Discussion

The experimental observations are accounted for by considering the following processes: (i) generation of triplet **1** spin polarized in enhanced absorption, (ii) ESPT to the **2** spin system, and (iii) RTPM polarization and spin lattice relaxation. These processes are examined in more detail before discussing the spectral features and their kinetics.

(i) Spin polarization of the photoexcited triplet state occurs because of the selectivity of intersystem crossing (ISC) from the first excited singlet state, due to spin−orbit interaction. For a triplet molecule in a fixed orientation with respect to the magnetic field, in the high field approximation ($B_0 \gg D/g\beta$, $E/g\beta$, where D and E are the zero field splitting parameters), ISC produces two opposite polarized EPR transitions. In a liquid solution of low viscosity, the net triplet polarization is obtained by averaging the polarization corresponding to all the possible molecular orientations. The following formula gives the polarization as a function of the populations of the triplet sublevels at zero field.[4]

$$P = \left(\frac{4}{15}g\beta B_0\right)[D(P_x + P_y - 2P_z) - 3E(P_x - P_y)] \quad (1)$$

The zero field splitting parameters D and E and the ratios of population rates P_x, P_y, and P_z of **1** were obtained from the triplet EPR spectrum recorded at 20 K in a rigid glass matrix. The following values fit the low-temperature experimental spectrum: $D = -9.45$ mT, $E = +0.65$ mT and $(P_x - P_z):(P_y - P_z) = 0.09:1.00$.[35] Substitution of these values in eq 1, gives the triplet polarization in enhanced absorption observed in solution ($P < 0$).

(ii) The triplet polarization is transferred to the free radical, which therefore initially appears in enhanced absorption.

(iii) The triplet and radical spin polarization is also affected by RTPM. A theoretical approach of the latter was presented some years ago,[36] based on the interaction of a free radical with a triplet molecule whose level populations are relaxed to the thermal equilibrium values. The principles of RTPM are the following: by collision of the triplet with a radical, an RTP is formed in one of the possible six spin states, which are split into a quartet and a doublet by the electron exchange interaction J. Because of the spin conservation in elementary steps of chemical reactions, the decay of the RTP into a singlet and a radical is allowed if the RTP is in the doublet state.

The efficiency of quartet−doublet transitions is higher when a quartet state Zeeman sublevel crosses a doublet one. The magnitude and sign of J determine which quartet and doublet sublevels do cross. When J is large and negative (doublet RTP at lower energy than quartet RTP) the level crossing occurs between $Q_{-3/2}$ and $D_{+1/2}$. This gives rise to selective population of the radical $|+^1/_2\rangle$ Zeeman state and emissive EPR line. Conversely, if J is positive, the involved levels are $Q_{+3/2}$ and $D_{-1/2}$ and the radical polarization is in enhanced absorption. For small values of J, $Q_{\pm 1/2}$, and $D_{\pm 1/2}$ become quasi-degenerate and the selective mixing depends on the hyperfine interaction and on the difference $(g_R - g_T)$ between the g factors of the radical and the triplet. In this case a multiplet effect arises: E/A if $J < 0$ or A/E if $J > 0$. In some cases superimposed net and multiplet polarization E*/A or A*/E were observed.[9,15,16,18,19]

It should be noted that RTPM alone does not account for the observed polarization in the TR-EPR spectrum of **2** in the early time after the laser pulse (see slice at 450 ns in Figure 3). In fact it is E/A*, which is not predicted in either assuming $J < 0$ or $J > 0$.

The time evolution of the radical ith line and of the triplet signal is accounted for by the solutions of the kinetic equations (2),[19] which include all the mentioned dynamic processes. They are:

$$\begin{aligned}
&\frac{\partial M_{yT}}{\partial t} = M_{zT}\omega_1 - M_{yT}\left(\frac{1}{T_{2T}} + \left(\frac{1}{\tau} + [R]k_q + [T]k_{TT}\right)\right)\\
&\frac{\partial M_{zT}}{\partial t} = -M_{yT}\omega_1 + (P_{eqT}[T] - M_{zT})\frac{1}{T_{1T}} - M_{zT}\left(\frac{1}{\tau} + [R]k_q + [T]k_{TT}\right) + P_{ESPTT}(P_{eqT}[T] - M_{zT})[R]k_q + P_{RTPMT}k_q[T][R]\\
&\frac{\partial M_{yRi}}{\partial t} = M_{zRi}\omega_1 - M_{yRi}\left(\frac{1}{T_{2Ri}} + [T]k_q\right)\\
&\frac{\partial M_{zRi}}{\partial t} = -M_{yRi}\omega_1 + (P_{eqRi}[R] - M_{zRi})\frac{1}{T_{1Ri}} + P_{ESPTRi}(P_{eqT}[T] - M_{zT})[R]k_q + P_{RTPMRi}k_q[T][R]\\
&\frac{\partial [T]}{\partial t} = -[T]\left(\frac{1}{\tau} + [R]k_q\right) - [T]^2k_{TT}
\end{aligned} \quad (2)$$

[R] is the concentration of **2**, which is assumed as a constant in the process, [T] is the time dependent concentration of **1** in the excited triplet state, and all the symbols bearing the subscript T or R are referred to the triplet or to the radical, respectively.

P_{eqRi} and P_{eqT} are the corresponding values of the radical and the triplet polarization at thermal equilibrium. The subscript i refers to those radicals giving the ith EPR line.

$\omega_1 = (g\beta/h)B_1$ is the Rabi frequency, which has the same value for the radical and triplet since the triplet signal is isotropic and analyzed by a Lorentzian line. k_q is the radical triplet quenching rate, k_{TT} is the triplet−triplet quenching rate, and $1/\tau$ is the rate of other decay processes. $M_{yRi/T}$, $M_{zRi/T}$, $T_{1Ri/T}$, and $T_{2Ri/T}$ have the usual meanings of magnetization components and relaxation times of the radical and triplet.

$P_{ESPT\,T}$ and $P_{RTPM\,T}$ represent respectively the rate of electron spin polarization transfer and the rate of triplet polarization due to RTPM.

The ESPT and RTPM constants for the radical, $P_{ESPT\,Ri}$ and $P_{RTPM\,Ri}$, are related to the previous ones by the relations:

$$P_{ESPT\,Ri} = -\frac{1}{3}P_{ESPT\,T}$$

$$\sum_i P_{RTPM\,Ri} = -P_{RTPM\,T} \qquad (3)$$

The first one takes into account the equal probability of polarization transfer from the triplet to each of the radical lines, while the second derives from the consideration that RTPM is only a spin sorting process and, overall, neither creates nor destroys magnetization.[19]

Computer simulations of the experimental signals were performed by solving numerically the above set of differential equations. As shown in Figure 3 the low field nitroxide line is only slightly superimposed with the triplet **1** signal and can be used as it is. Conversely, for the simulation of the other two radical lines the triplet signal contribution has to be subtracted. The curves of Figure 4, together with the calculated fit, represent the time evolution after having done the subtraction.

The parameters used in the fitting are the microwave Rabi frequency ω_1, which was determined by measuring in the same cavity the nutation frequency for a triplet C_{60} derivative in glassy matrix at 120−130 K. In these conditions the Rabi frequency is $\sqrt{2}\omega_1$. The concentration of **2**, [R], and the initial concentration of triplet states, c_0, were taken as fixed parameters. The latter is estimated by considering the laser light intensity, the solution absorption coefficient at the laser wavelength, and the triplet yield, which is about unity. c_0 corresponds to 1% of the triplet precursor fullerene concentration.

M_{y0Ri} and M_{z0Ri} were obtained from the stationary solution of the Bloch equations for the radical magnetization in the presence of the microwave field $B_1 = \omega_1/\gamma$.

P_{eqT} is a scale factor; if it is set equal to unity, the equilibrium polarization of the radical P_{eqR} is $^3/_8$.

The triplet lifetime τ due to processes other than the quenching by the radical, the triplet relaxation times T_1 and T_2, and the triplet−triplet annihilation rate constant k_{TT}[37] were obtained by fitting the decay curve of **1** recorded in the absence of **2** by setting [R] = 0 in eqs 2. The values $\tau = 4.8\ \mu$s, $T_1 = 0.670\ \mu$s, and $T_2 = 0.080\ \mu$s were obtained. These values of τ, T_1, and T_2 were used for the **1** + **2** system calculations.

M_{z0T} is the triplet magnetization at zero time, that is, just after the laser pulse, ISC, and sublevel population averaging due to fast triplet molecule rotational diffusion. Even if in principle M_{z0T} could be obtained from eq 1, we have used it as a variable to fit the experimental data. We obtained $M_{z0T} = 5c_0P_{eqT}$. From eq 1, using the D and E parameters and the populating rate ratios measured in the toluene rigid matrix and given above, one obtains the same value. This provides a very good internal check.

TABLE 1: Parameters Employed for Fitting Experimental Curves of a 2 mM Solution of 1 and 2 in $CHCl_3$

	radical low field line	radical central line	radical high field line	triplet line
T_1 (μs)	0.260	0.260	0.260	0.670
T_2 (μs)	0.050	0.050	0.050	0.080
k_q ($M^{-1}\,s^{-1}$)		5×10^7		
P_{ESPT} (P_{eqT})	2.7	2.7	2.7	−8.1
P_{RTPM} (P_{eqT})	−4.7	−3.1	−0.7	8.5

The other adjustable parameters were taken in order to simultaneously fit the three radical lines and the triplet line time evolution. They are reported in Table 1.

T_1 of the nitroxide obtained from the fit is in line with the values reported in the literature for radicals of this type.[19,38]

The polarization factors P_{RTPM} are quite similar to the value reported for the C_{60}/TEMPO system.[19]

From the polarization of the three ^{14}N hyperfine components, P_{-1}, P_0, and P_1, we can separate the net and multiplet effect contributions. The multiplet effect is $(P_{-1} - P_1)/2 = 2$, while the net effect is $(P_{-1} + P_1)/2 = -2.7$. This latter derives from the radical triplet interaction in the narrow $Q_{-3/2}$ and $D_{+1/2}$ level crossing region and, if the radical and the triplet g values are different, from the interaction in the region were the $D_{\pm1/2}$ and $Q_{\pm1/2}$ levels are almost degenerate. In the radical **2**/triplet **1** system $\Delta g = 4 \times 10^{-3}$. At the 0.33 T magnetic field value of the X band spectrometer the Δg contribution is expected to be of the order of one-half the multiplet effect.

Finally, the triplet quenching rate constant ($k_q = 5 \times 10^7\ M^{-1}\,s^{-1}$) obtained by assuming that 1% of **1** is photoexcited in the triplet state ($c_0 = 2 \times 10^{-5}$) results to be much lower than the diffusion-controlled rate constant, which at 260 K in chloroform ($\eta = 0.83$ cP)[39] is expected to be $7.2 \times 10^9\ M^{-1}\,s^{-1}$. A diffusion-controlled rate constant was obtained for the triplet quenching reaction of pristine C_{60} by TEMPO radicals.[19] Contrary to the latter system, in our case the quenching reaction should be determined by entropic factors due to the requirement of a correct approach of the two reaction partners, because the triplet excitation is localized on the fullerene ball, which bears a bulky crown ether addend. The radical **2** also has a rather bulky substituent on the opposite side of the radical center. However, similar rate constants were obtained using the TEMPO radical, indicating that steric hindrance of the radical has little effect.

For phthalocyanine/TEMPO systems, k_q was obtained from a kinetic treatment of the radical and triplet signal decay, without taking into account the microwave field. Values similar to or even smaller than those in our case were obtained.[32,40]

Conclusions

A [60]fullerene adduct illuminated by laser light in chloroform solution containing a nitroxide radical shows TR-EPR spectra with intense spin-polarized spectral lines due to both species: the free radical and the fullerene derivative in its first excited triplet state. Because of the small zero field splitting parameters of the fullerene triplet and the highly selective population of the triplet sublevels, this displays a quite narrow and spin-polarized line that allows for precise analysis.

The spin polarization of the excited triplet and of the free radical and their time evolution are quantitatively accounted for by a faster contribution arising by ESPT from the triplet to the radical, and a slower one due to RTPM.

Acknowledgment. This work was supported by MURST (Contract No. MM03198284). We thank Prof. Michele Maggini of the Department of Organic Chemistry of the University of Padova for helpful discussions.

References and Notes

(1) Salikhov, K. M.; Molin, Y. N.; Sagdeev, R. Z.; Buchachenko, A. L. In *Spin Polarisation and Magnetic Effects in Radical Reactions*; Molin, Y., Ed.; Elsevier: Amsterdam, 1984; p 324.

(2) Hirota, N.; Yamauchi, S. In *Dynamic Spin Chemistry*; Nagakura, S., Hayashi, H., Azumi, T., Eds.; Wiley: New York, 1998; pp 187−248.

(3) *Chemically Induced Magnetic Polarisation*; Muus, L. T., Atkins, P. W., McLauchlan, K. A., Pedersen, J. B., Eds.; Reidel: Dordrecht, The Netherlands, 1977.

(4) Wong, S. K.; Hutchinson, D. A.; Wan, J. K. S. *J. Phys. Chem.* **1973**, *58*, 985.

(5) Kaptein, R. *J. Am. Chem. Soc*. **1972**, *94*, 6251.

(6) Adrian, F. J. *J. Chem. Phys.* **1971**, *54*, 3918.

(7) Pedersen, J. B.; Freed, J. H. *J. Chem. Phys.* **1975**, *62*, 1706.

(8) Blättler, C.; Jent, F.; Paul, H. *Chem. Phys. Lett.* **1990**, *166*, 375.

(9) Kawai, A.; Okutsu, T.; Obi K. *J. Phys. Chem.* **1991**, *95*, 9130.

(10) Jenks, W. S.; Turro, N. J. *J. Am. Chem. Soc*. **1990**, *112*, 9009.

(11) Porter, G.; Wright, M. R. *Discuss. Faraday Soc*. **1959**, *27*, 18.

(12) Hoytink, G. J. *Mol. Phys.* **1969**, *2*, 114.

(13) Birks, J. B. In *Photophysics of Aromatic Molecules*; Birks, J. B, Ed.; John Wiley: London, 1970; pp 447−449.

(14) Swenberg, C. E.; Geacintov, N. E. In *Organic Molecular Photophysics*; Birks, J. B., Ed.; John Wiley: London, 1973; pp 498−499.

(15) Kawai, A.; Obi, K. *J. Phys. Chem.* **1992**, *96*, 52.

(16) Kawai, A.; Obi, K. *J. Phys. Chem.* **1992**, *96*, 5701.

(17) Samanta, A.; Kamat, P. V. *Chem. Phys. Lett.* **1992**, *199*, 635.

(18) Goudsmit, G.-H.; Paul, H.; Shushin, A. I. *J. Phys. Chem.* **1993**, *97*, 13243.

(19) Goudsmit, G.-H.; Paul, H. *Chem. Phys. Lett.* **1993**, *208*, 73.

(20) Kobori, Y.; Kawai, A.; Obi, K. *J. Phys. Chem.* **1994**, *98*, 642.

(21) Kobori, Y.; Takeda, K.; Tsuji, K.; Kawai, A.; Obi, K. *J. Phys. Chem A* **1998**, *102*, 5160.

(22) Corvaja, C.; Maggini, M.; Ruzzi, M.; Scorrano, G.; Toffoletti, A. *Appl. Magn. Reson.* **1997**, *12*, 477.

(23) Corvaja, C.; Franco, L.; Toffoletti, A. *Appl. Magn. Reson.* **1994**, *7*, 257.

(24) Corvaja, C.; Maggini, M.; Prato, M.; Scorrano, G.; Venzin, M *J. Am. Chem. Soc.* **1995**, *117*, 8857.

(25) Ishii, K.; Fujisawa, J.; Ohba, Y.; Yamauchi, S. *J. Am. Chem. Soc.* **1996**, *118*, 13079.

(26) Corvaja, C.; Sartori, E.; Toffoletti, A.; Formaggio, F.; Crisma, M.; Toniolo, C.; Mazaleyrat, J.; Wakselman, M. *Chem. Eur. J.* **2000**, *6*, 2775.

(27) Sartori, E.; Garlaschelli, G.; Toffoletti, A.; Corvaja, C.; Maggini, M.; Scorrano, G. *Chem. Commun.* **2001**, 311.

(28) Imamura, T.; Onitsuka, O.; Obi, K. *J. Phys. Chem.* **1986**, *90*, 6741.

(29) Jenks, W. S.; Turro, N. J. *Res. Chem. Intermed.* **1990**, *13*, 237.

(30) Fujisawa, J.; Ishi, K.; Ohba, Y.; Iwaizumi, M.; Yamauchi, S. *J. Phys. Chem.* **1995**, *99*, 17082.

(31) Ishi, K.; Fujisawa, J.; Ohba, Y.; Yamauchi, S. *J. Phys. Chem. A* **1997**, *101*, 434.

(32) Saiful, I. S. M; Fujisawa, J.; Kobayashi, N.; Ohba, Y.; Yamauchi, S. *Bull. Chem. Soc. Jpn.* **1999**, *72*, 661.

(33) Blank, A.; Levanon, H. *J. Phys. Chem. A* **2000**, *104*, 794.

(34) Hankovszky, H. O.; Hideg, K.; Lex, L. *Synthesis* **1981**, 147.

(35) The sign of D cannot be obtained from the experiment. It is assumed negative as for $^3C_{60}$.

(36) Shushin, A. I. *Z. Phys. Chem.* **1993**, *182*, 9.

(37) In our conditions the triplet−triplet annihilation process does not affect appreciably the decay of the triplet.

(38) Percival, P. W.; Hyde, J. S. *J. Magn. Resonance* **1976**, *23*, 249.

(39) Yaws, C. L. *Handbook of viscosity*; Gulf Publishing Company: Houston, 1995; vol. 1, p 16.

(40) It should be noted that in order to compare k_q of ref 32 and the value reported in Table 1, the latter should be multiplied by the factor P_{RTPM}. Also electron spin transfer rate constant k_{ESPT} of ref 32 has very similar value as k_qP_{ESPT}.